grals are neglected as a result of the screening techniques (Fig. 5). Thus, a mere ~1.5% of all interactions in this molecule are treated by analytic integration. However, this computation is costly (Fig. 4).

In the GFMM, the separation between NF and FF is done in terms of uncontracted Gaussian functions because the product of two contracted Gaussians gives a linear combination of Gaussian distributions with different exponents centered at different points. The range criterion explained above thus has to be individually applied to these charge distributions. On the other hand, modern Gaussian integral packages, and in particular the PRISM algorithm (*10*) used in the Gaussian program (*8*), utilize contracted basis sets, thereby significantly reducing the computational cost of evaluating integrals over the uncontracted set. We estimate (Figs. 4 and 5) that calculating NF integrals over uncontracted rather than contracted functions for the 3-21G basis increases the computational cost by a factor of 5. This factor imposes a lower bound on the percentage of interactions that must be included in the FF for the GvFMM to become competitive with analytic integration. Given an overhead factor of 5 and neglecting the cost of FF evaluation, the GvFMM would be more expensive than analytic integration whenever more than 20% of all interactions were included in the NF. In our benchmarks, this break-even point is achieved at small molecular size (Fig. 5).

In a timing comparison in a fully uncontracted basis set, the GvFMM became as much as 50 times faster than analytic integration for fairly small-size molecular systems. All results reported in this paper were obtained with contracted bases, because these are commonly used in practical calculations. These results, although limited to benchmark graphene-sheets, are also valid for more complex materials. Given the speed, accuracy, and scaling properties of the GvFMM in practical, high-accuracy calculations, this method appears very promising for future electronic structure calculations on large molecular systems.

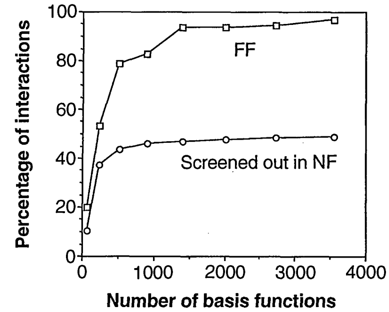

Fig. 5. (☐) Percentage of interactions (uncontracted two-electron integrals) included in the FF component of the GvFMM (for the optimum box-size distribution used in Fig. 2) and treated by the tree hierarchy. (○) Percentage of uncontracted two-electron integrals that were prescreened and neglected in the NF portion of the Coulomb problem using empirical and mathematical bounds.

REFERENCES AND NOTES

1. L. Greengard, *Science* **265**, 909 (1994); ——— and V. Rokhlin, *J. Comput. Phys.* **73**, 325 (1987).
2. L. Greengard, *The Rapid Evaluation of Potential Fields in Particle Systems* (MIT Press, Cambridge, MA, 1988).
3. C. A. White and M. Head-Gordon, *J. Chem. Phys.* **101**, 6593 (1994); H. Ding, N. Karasawa, W. A. Goddard III, *ibid.* **97**, 4309 (1992); J. Shimada, H. Kaneko, T. Takada, *J. Comput. Chem.* **15**, 28 (1994).
4. C. A. White, B. G. Johnson, P. M. W. Gill, M. Head-Gordon, *Chem. Phys. Lett.* **230**, 8 (1994).
5. H. G. Petersen, D. Soelvason, J. W. Perram, E. R. Smith, *J. Chem. Phys.* **101**, 8870 (1994); *Proc. R. Soc. London Ser. A* **448**, 389 (1995).
6. S. F. Boys, *Proc. R. Soc. London Ser. A* **200**, 542 (1950).
7. The technical details of our present implementation, and an extensive study of the method's accuracy and speed, will be reported elsewhere. We prefer the name "Gaussian FMM" over "continuous FMM" [as in (*4*)] to underscore the fact that (i) the product of two Gaussian orbitals is a sum of well-localized Gaussian charge distributions amenable to efficient treatment by FMM, which is not true for other continuous charge distributions, and (ii) the error bound discussed here derives from and applies exclusively to Gaussian distributions.
8. Gaussian 95, Development version; M. J. Frisch *et al.*, Gaussian, Inc., Pittsburgh, PA.
9. D. L. Strout and G. E. Scuseria, *J. Chem. Phys.* **102**, 8448 (1995).
10. P. M. W. Gill and J. A. Pople, *Int. J. Quantum Chem.* **40**, 753 (1991).

11. This work was supported by the Air Force Office of Scientific Research (grant F49620-95-1-0203), the National Science Foundation (CHE-9321297), the Welch Foundation, and Gaussian, Inc. G.E.S. is a Camille and Henry Dreyfus Teacher-Scholar.

22 August 1995; accepted 30 October 1995

Low-Compressibility Carbon Nitrides

David M. Teter and Russell J. Hemley

First-principles calculations of the relative stability, structure, and physical properties of carbon nitride polymorphs predict a cubic form of C_3N_4 with a zero-pressure bulk modulus exceeding that of diamond. Like diamond, this new phase could potentially be synthesized at high pressure and quenched to ambient pressure for use as a superhard material. The calculations also predict that α-C_3N_4 and graphite-C_3N_4 are energetically favored relative to β-C_3N_4 and that published diffraction data can be re-indexed as α-C_3N_4 with lower error.

Intense theoretical and experimental interest has been focused on the possibility of new low-compressibility materials with bulk moduli and hardness exceeding that of diamond. Carbon nitrides have been proposed as superhard materials on the basis of empirical systematics (*1*). First-principles calculations have suggested that a hypothetical material, β-C_3N_4, may have a bulk modulus somewhat lower than that of diamond (*2*, *3*). These results have motivated theoretical calculations (*4–8*) and experimental efforts to synthesize and characterize this compound (*10–20*). Amorphous C-N films have been synthesized (*14*, *16*, *20*), and small crystallites have been found in some of these films (*15*, *17–19*). Electron diffraction patterns of these crystallites were indexed as the β-C_3N_4 structure. However, these data can also be fit to carbon phases (*9*). Other forms of carbon nitride with high hardness have been suggested, including a fullerene-like carbon nitride (*21*) and a crystalline carbon nitride composite (*22*). In this report, we investigate the stability and properties of carbon nitrides using first-principles calculations and show that α-C_3N_4 and graphite-C_3N_4 are energetically preferred over β-C_3N_4 and describe a cubic form of C_3N_4 that may have a zero-pressure bulk modulus (K_0) exceeding that of diamond and be metastable at zero pressure.

Assuming that a low-energy carbon nitride structure with a high bulk modulus must have carbon four-coordinated with nitrogen, and nitrogen three-coordinated with carbon, we have identified several additional prototype structures by considering chemical systems with this type of bonding topology and by locating dense structures in these systems. Using first-principles pseudopotential total energy techniques (*23*), we examined a series of C_3N_4 polymorphs to determine their energetics, structure, and physical properties, including K_0, density, and band gap.

Our calculations, like those in earlier studies of carbon nitride (*4–7*), were carried out using density-functional techniques within the local density approximation (LDA) to electron exchange and correlation. We used a preconditioned conjugate-gradient method to minimize the electronic degrees of freedom. The electronic wave

---

D. M. Teter, Geophysical Laboratory and Center for High Pressure Research, Carnegie Institution of Washington, Washington, DC 20015, USA, and Department of Materials Science and Engineering, Virginia Tech, Blacksburg, VA, 24061, USA.
R. J. Hemley, Geophysical Laboratory and Center for High Pressure Research, Carnegie Institution of Washington, 5251 Broad Branch Road, NW, Washington, DC, 20015, USA.

functions were expanded in a plane-wave basis set with periodic boundary conditions. We used extended norm-conserving and hardness-conserving (ENHC) pseudopotentials (*24*). This scheme ensures that the total energies of the atom and pseudoatom match to second order with respect to arbitrary changes in valence-state occupancy. This additional condition has been shown to improve pseudopotential transferability in studies of diamond-carbon (*24*), silica (*25*), and the linear response properties of free atoms (*26*). For each structure, we calculated the total energy over a wide range of volumes. At a given volume, we determined the positions of the cations and the anions by minimizing the forces on the ions, and the unit cell edges were determined by minimizing the stress on the cell. We fit the resulting energies to a Birch equation of state (*27*) to calculate the pressure, K_0, and pressure derivative of the bulk modulus (K'_0).

The β-C_3N_4 structure is based on the β-Si_3N_4 structure, with C substituted for Si. This structure is similar to the phenacite (Be_2SiO_4) structure and consists of fourfold coordinated carbon linked by threefold coordinated N atoms into a network of three-, four- and sixfold rings of CN_4 tetrahedra (Fig. 1A). The unit cell contains 14 atoms and has $P3$ symmetry. The α-C_3N_4 structure can be described as an ABAB . . . stacking sequence of layers of β-C_3N_4 (A) and its mirror image (B). The unit cell contains 28 atoms and has $P3_1c$ symmetry (Fig. 1B). When the symmetry of the optimized $P3_1c$ structure was relaxed to $P3$, there were no changes in the atomic coordinates of the structure. The graphitic form of carbon nitride consists of an ABAB . . . stacking of the planar structure (*28*) (Fig. 1C). The unit cell contains 14 atoms and exhibits $P\bar{6}m2$ symmetry. Another candidate suggested by this analysis is the pseudocubic α-$CdIn_2Se_4$ structure (*31*) (Fig. 1D). This structure can be classified as a defect-zincblende structure type, a structure type previously predicted for C_3N_4 by Liu *et al.* (*6*). It exhibits $P\bar{4}2m$ symmetry and contains seven atoms in the unit cell. We also searched for possible candidate structures in the Zn_2SiO_4 system, because the zero-pressure willemite-I structure is isomorphous with that of phenacite. In a study of high-pressure transformations in zinc silicates, Syono *et al.* found that the willemite-I structure transforms to the willemite-II structure at 3 GPa at 1400°C and can be quenched to ambient conditions (*29*). The willemite-II structure exhibits $I\bar{4}2d$ symmetry and has 28 atoms in the unit

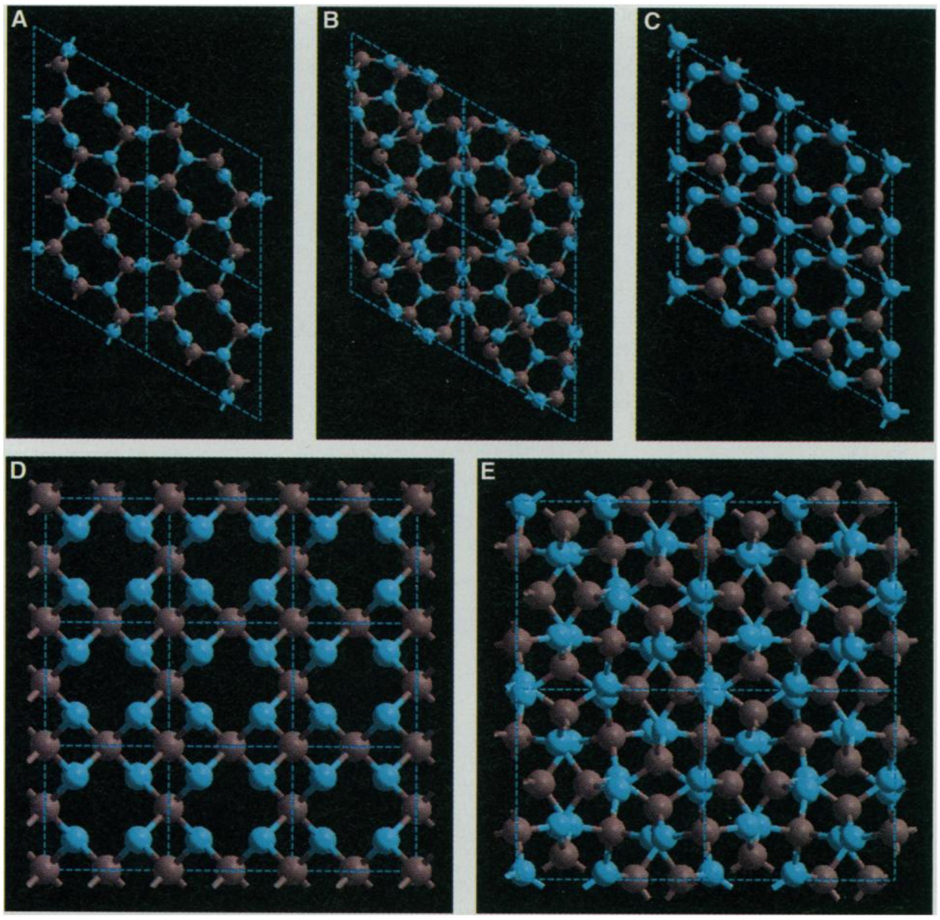

Fig. 1. Representation of the β-C_3N_4 (**A**), α-C_3N_4 (**B**), graphite-C_3N_4 (**C**), pseudocubic-C_3N_4 (**D**), and cubic-C_3N_4 (**E**) structures down the [001] axis. The carbon and nitrogen atoms are depicted as gray and blue spheres, respectively.

Table 1. Equilibrium structural parameters, bulk moduli, and total energies calculated for α-C_3N_4, β-C_3N_4, cubic-C_3N_4, pseudocubic-C_3N_4, and graphite-C_3N_4. The differences in total energies are converged to below 0.008 eV per C_3N_4 unit with respect to *k*-point integration and kinetic energy cutoff. The calculations were completed at a kinetic energy cutoff of 60 Hartrees. The structural parameters were considered to be fully relaxed when the forces on the ions were less than 0.02 eV/Å and all Pulay-corrected stress tensor components were less than 0.002 eV/Å^3.

	α-C_3N_4	β-C_3N_4	Cubic-C_3N_4	Pseudocubic-C_3N_4	Graphitic-C_3N_4
Space group	$P3_1c$ (159)	$P3$ (143)	$I\bar{4}3d$ (220)	$P\bar{4}2m$ (111)	$P\bar{6}m2$ (187)
Z	4	2	4	1	2
a (Å)	6.4665	6.4017	5.3973	3.4232	4.7420
c (Å)	4.7097	2.4041			6.7205
$C1$	(0.5171, 0.0813, 0.2102)	(0.7732, 0.1784, 0.2499)	(0.8750, 0.0000, 0.2500)	(0.0000, 0.0000, 0.0000)	(0.3517, 0.1759, 0.0000)
$C2$	(0.1656, 0.2547, 0.9905)	(0.2271, 0.8216, 0.7501)		(0.5000, 0.0000, 0.5000)	(0.0197, 0.5099, 0.5000)
$N1$	(0.0000, 0.0000, 0.0000)	(0.3333, 0.6667, 0.7500)	(0.2812, 0.2812, 0.2812)	(0.2454, 0.2454, 0.2547)	(0.0000, 0.0000, 0.0000)
$N2$	(0.3333, 0.6667, 0.6278)	(0.6667, 0.3333, 0.2500)			(0.6667, 0.3333, 0.5000)
$N3$	(0.3471, 0.9510, 0.9706)	(0.0331, 0.3309, 0.2502)			(0.1694, 0.3387, 0.5000)
$N4$	(0.3148, 0.3188, 0.2423)	(0.9669, 0.6705, 0.7498)			(0.5026, 0.4974, 0.0000)
$\rho_{n,0}$ (atom-mol/cm^3)	0.2726	0.2724	0.2957	0.2897	0.1776
K_0 (GPa)	425	451	496	448	—
K'_0	3.1	3.3	3.4	3.4	—
E_0 (eV/unit)	−1598.669	−1598.403	−1597.388	−1597.225	−1598.710

cell. The cubic-C_3N_4 we studied in this work is based on the high-pressure willemite-II structure (*30*) of Zn_2SiO_4. When C was substituted for Zn and Si, and N was substituted for O, it was found that this structure adopts cubic $I\bar{4}3m$ symmetry when the structure is allowed to relax (Fig. 1E).

All of the tetrahedrally coordinated structures exhibit similar C–N bond lengths and intertetrahedral C–N–C and intratetrahedral N–C–N bond angles (Table 1). As shown in Fig. 2, α-C_3N_4 is predicted to have a lower energy than β-C_3N_4 at all volumes. We find that diffraction data (*15, 17, 18*) can be re-indexed as α-C_3N_4 with lower root-mean-square error. This result agrees with earlier work by Guo and Goddard (*8*) using interatomic potentials. As shown in Fig. 2, the graphite-C_3N_4 structure is predicted to have a slightly lower energy than α-C_3N_4. This result agrees qualitatively with earlier calculations comparing the energetics of planar-C_3N_4 to those of β-C_3N_4 (*6, 7*). This structure should be a good candidate precursor for the high-pressure synthesis of C_3N_4 compounds.

The zero-pressure cubic-C_3N_4 structure is higher in energy than both α- and β-C_3N_4, but became the energetically favorable structure as the volumes were decreased. We predicted that the transition pressure from α- to cubic-C_3N_4 is approximately 68 GPa. The predicted transition pressure from graphite-C_3N_4 to cubic-C_3N_4 is approximately 12 GPa, which can be easily attained using large volume presses.

For the cubic-C_3N_4 structure, the calculated K_0 is 496 GPa, which is greater than the experimental K_0 of diamond of 442 GPa (*32*). These results suggest that cubic-C_3N_4 may also exhibit high hardness (*33*). In order to assess the mechanical stability of cubic-C_3N_4, we displaced the internal coordinates at a variety of volumes. The atoms returned to their initial positions following energy minimization under $P1$ symmetry. Hence the structure is predicted to be mechanically stable at high pressures as well as at ambient pressures. We also determined the elastic constants of cubic-C_3N_4 using established first-principles techniques (*34*). The structure meets the Born stability criteria for mechanical stability (*35*).

The widespread interest in carbon nitrides also arises from their predicted wide band gap and high atomic density. The calculated band gap of the cubic-C_3N_4 phase is 2.90 eV. For α-C_3N_4 and β-C_3N_4 the calculated band gaps are 3.85 and 3.25 eV, respectively. In all cases, the gap is found to be indirect. Because LDA usually underestimates experimental band gaps by 15 to 20%, the actual band gaps of the carbon nitride structures, if they can be synthesized, should be higher. All of these phases except graphite-C_3N_4 have predicted atomic densities approaching that of diamond (experimental result: 0.2950 mol-atoms/cm^3; LDA result: 0.3007 mol-atoms/cm^3). We find that the atomic density of cubic-C_3N_4 is 0.2957 mol-atoms/cm^3.

On the basis of the high atomic density and bonding topology of this structure, cubic-C_3N_4 should be an excellent thermal conductor. Most experimental studies of carbon nitrides have been carried out at ambient or low-pressure conditions. Our results indicate that high-pressure synthesis should be important in the search for new carbon nitrides. The calculated transition pressure to the cubic-C_3N_4 phase from low-pressure phases (graphite-C_3N_4 or α-C_3N_4) is within reach of modern high-pressure techniques. Moreover, the predicted transition pressure for synthesis of cubic-C_3N_4 from the graphite-C_3N_4 phase is within the reach of large volume presses, which would allow synthesis at an industrial scale. Our results suggest that it may also be possible to synthesize other high-pressure carbon nitrides with low compressibility (for example, pseudocubic-C_3N_4) as pressure-quenchable metastable phases.

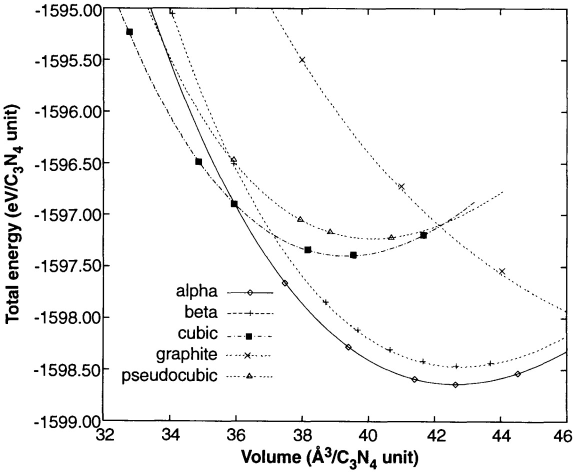

Fig. 2. Total energies as a function of volume for the structures studied. The curves were generated from fits to the calculated data points using the Birch equation of state. For the α-C_3N_4 structure, we predict a K_0 of 425 GPa. For the β-C_3N_4 structure, the K_0 is 451 GPa and does not change significantly when the symmetry constraints are lowered from $P6_3/m$ to $P3$. The K_0 for pseudocubic-C_3N_4 structure is also high (448 GPa); although this phase does not appear to be energetically favorable relative to α-C_3N_4 and cubic-C_3N_4, it is conceivable that this material could be formed metastably. Transition pressures were determined by taking common tangents.

REFERENCES AND NOTES

1. M. L. Cohen, *Phys. Rev. B* **32**, 7988 (1985).
2. A. Y. Liu and M. L. Cohen, *Science* **245**, 841 (1989).
3. ______, *Phys. Rev. B* **41**, 10727 (1990).
4. J. L. Corkill and M. L. Cohen, *ibid.* **48**, 17622 (1993).
5. H. Yao and W. Y. Ching, *ibid.* **50**, 11231 (1994).
6. A. Y. Liu and R. M. Wentzcovitch, *ibid.*, p. 10362.
7. J. Ortega and O. F. Sankey, *ibid.* **51**, 2624 (1995).
8. Y. Guo and W. A. Goddard, *Chem. Phys. Lett.* **237**, 72 (1995).
9. J. V. Badding and D. C. Nesting, *Chem. Mater.*, in press.
10. T. Sekine, H. Kanda, Y. Bando, M. Yokohama, K. Hojou, *J. Mat. Sci. Lett.* **9**, 1376 (1990).
11. L. Maya, D. R. Cole, E. W. Hagaman, *J. Am. Ceram. Soc.* **74**, 1686 (1991).
12. M. Wixom, *ibid.* **73**, 1973 (1990).
13. J. J. Cuomo, P. A. Leary, D. Yu, W. Reuter, M. Frisch, *J. Vac. Sci. Technol.* **16**, 299 (1976).
14. H. X. Han and B. J. Feldman, *Solid State Commun.* **65**, 921 (1988).
15. C. Niu, Y. Z. Liu, C. M. Lieber, *Science* **261**, 334 (1993).
16. D. Marton, K. J. Boyd, A. H. Al-Bayati, S. S. Todorov, J. W. Rabalais, *Phys. Rev. Lett.* **73**, 118 (1994).
17. K. M. Yu, M. L. Cohen, E. E. Haller, W. L. Hansen, A. Y. Lu, I. C. Wu, *Phys. Rev. B* **49**, 5034 (1994).
18. J. P. Riviere, D. Texier, J. Delafond, M. Jaouen, E. L. Mathe, J. Chaumont, *Mater. Lett.* **22**, 115 (1995).
19. Z. M. Ren *et al.*, *Phys. Rev. B* **51**, 5274 (1995).
20. Y. Yang, K. A. Nelson, F. Adibi, *J. Mater. Res.* **10**, 41 (1995).
21. H. Sjostrom, M. Stafstrom, J. E. Sundgren, *Phys. Rev. Lett.* **75**, 1336 (1995).
22. D. Li *et al.*, *Appl. Phys. Lett.* **67**, 203 (1995).
23. M. C. Payne, M. P. Teter, D. C. Allan, T. A. Arias, J. D. Joannopoulos, *Rev. Mod. Phys.* **64**, 1045 (1992).
24. M. P. Teter, *Phys. Rev. B* **48**, 5031 (1993).
25. D. M. Teter, G. V. Gibbs, M. B. Boisen, D. C. Allan, M. P. Teter, *Phys. Rev. B* **52**, 8064 (1995).
26. A. Filippetti, D. Vanderbilt, W. Zhong, Y. Cai, G. B. Bachelet, *ibid.*, p. 11793.
27. F. Birch, *J. Geophys. Res.* **83**, 1257 (1978).
28. J. Kouvetakis, A. Bandari, M. Todd, B. Wilkens, N. Cave, *Chem. Mater.* **6**, 1376 (1994).
29. Y. Syono, S. Akimoto, Y. Matsui, *J. Solid State Chem.* **3**, 369 (1971).
30. F. Marumo and Y. Syono, *Acta. Crystallogr.* **B27**, 1868 (1971).
31. P. P. Lottici, G. Antonioli, C. Razzetti, *J. Chem. Phys. Solids* **50**, 967 (1989).
32. Our LDA results at the same level of theory and convergence calculate a diamond K_0 of 468 GPa. While the predicted bulk moduli of other hypothetical materials, including the high-pressure BC-8 carbon structure, approach that of diamond, the cubic-C_3N_4 K_0 exceeds it.
33. Although a rigorous correlation between bulk modulus and hardness does not exist, it is found empirically that for an isotropic material, hardness is usually proportional to K_0, assuming the absence of plastic deformation. Hence, the hardness of cubic-C_3N_4 may exceed that of diamond.
34. M. J. Mehl, *Phys. Rev. B* **47**, 2493 (1993).
35. We determined the elastic constants of cubic-C_3N_4 using norm-conserving Troullier and Martins pseudopotentials at a kinetic energy cutoff of 25 Hartrees with a [444] Monkhorst Pack grid. We found c_{11} = 863 GPa, c_{12} = 313 GPa, and c_{44} = 348 GPa. This meets the Born mechanical stability criteria for a cubic crystal, as c_{11}, c_{11}-c_{12}, and c_{44} are all positive.
36. We thank M. T. Stawovy, O. F. Sankey, M. O'Keeffe, L. W. Finger, R. M. Hazen, C. T. Prewitt, and J. V. Badding for comments. Computational results were obtained using a version of the software program Plane-Wave from Biosym Technologies of San Diego.

26 September 1995; accepted 22 November 1995